

Article

Climate–Growth Relationships in *Laurus azorica*—A Dominant Tree in the Azorean Laurel Forest

Diogo C. Pavão ^{1,2,3,4,*} , Jernej Jevšenak ^{5,6} , Lurdes Borges Silva ^{1,3,4}, Rui Bento Elias ⁷  and Luís Silva ^{1,2,3,4} 

- ¹ CIBIO, Centro de Investigação em Biodiversidade e Recursos Genéticos, InBIO Laboratório Associado, Pólo dos Açores, Universidade dos Açores, Campus de Ponta Delgada, Rua da Mãe de Deus, 9500-321 Ponta Delgada, Portugal
 - ² Faculty of Sciences and Technology, University of the Azores, Campus de Ponta Delgada, Rua da Mãe de Deus, 9500-321 Ponta Delgada, Portugal
 - ³ BIOPOLIS Program in Genomics, Biodiversity and Land Planning, CIBIO, Campus de Vairão, 4485-661 Vairão, Portugal
 - ⁴ UNESCO Chair—Land Within Sea: Biodiversity & Sustainability in Atlantic Islands
 - ⁵ TUM School of Life Sciences, Technical University of Munich, D-85354 Freising, Germany
 - ⁶ Department for Forest and Landscape Planning and Monitoring, Slovenian Forestry Institute, 1000 Ljubljana, Slovenia
 - ⁷ cE3c—Centre for Ecology, Evolution and Environmental Changes, Azorean Biodiversity Group, CHANGE—Global Change and Sustainability Institute, Faculty of Agricultural and Environmental Sciences, University of the Azores, Rua Capitão João d’Ávila, Pico da Urze, 9700-042 Angra do Heroísmo, Portugal
- * Correspondence: diogo.c.pavao@uac.pt

Abstract: Forests on oceanic islands, such as the Azores archipelago, enable interesting dendroclimatic research, given their pronounced climatic gradients over short geographical distances, despite the less pronounced seasonality. The Lauraceae play an essential ecological role in Macaronesian natural forests. An example is *Laurus azorica* (Seub.) Franco, a relevant species given its high frequency and physiognomic dominance in Azorean laurel forests. This study aims to quantify climate–growth relationships in *L. azorica* using a dendroecological approach. We sampled four stands at São Miguel and two stands at Terceira islands, for a total of 206 trees. Following standard dendrochronological methods and rigorous sample selection procedures, we obtained relatively low r_{bar} values and high temporal autocorrelation. Using a stepwise Random Forest analysis followed by Generalized Linear Models calculation, we found prominent effects of present and previous year temperature, but a low precipitation signal on growth rings, with some model variation between stands. Our results agreed with previous observations for broad-leaved species with diffuse porous wood, contributing to increase the baseline dendroecological knowledge about Azorean forests. Due to the high levels of within- and between-stand variation, and to refine the climatic signal analysis, complementary approaches should be explored in the future.

Keywords: Azores; dendroclimatology; generalized linear models; laurel forest; Macaronesia; random forest



Citation: Pavão, D.C.; Jevšenak, J.; Silva, L.B.; Elias, R.B.; Silva, L. Climate–Growth Relationships in *Laurus azorica*—A Dominant Tree in the Azorean Laurel Forest. *Forests* **2023**, *14*, 166. <https://doi.org/10.3390/f14020166>

Academic Editors: Baozhang Chen and Yu Liu

Received: 22 November 2022

Revised: 3 January 2023

Accepted: 12 January 2023

Published: 17 January 2023



Copyright: © 2023 by the authors. Licensee MDPI, Basel, Switzerland. This article is an open access article distributed under the terms and conditions of the Creative Commons Attribution (CC BY) license (<https://creativecommons.org/licenses/by/4.0/>).

1. Introduction

Oceanic islands, particularly those of volcanic origin, are usually distinguished by their peculiar and heterogeneous environments [1–4]. These ecosystems have been the focus of research in biogeography, plant ecology, and, more recently, dendrochronology. Orographic precipitation regimes and complex topography lead to considerable spatial variation in temperature and water availability, facilitating studies of climate–growth relationships across environmental gradients [4–7], and allowing us to better understand the potential impact of a shifting climate on island species. Nevertheless, wood anatomy and growth dynamics of forest trees in oceanic islands remain largely underexplored [8–15], particularly in Macaronesia [10,11,13,14,16–19], a biogeographic region including North Atlantic

archipelagos that encompass a wide breadth of climatic conditions. Those archipelagos constitute a hotspot of plant diversity, with laurel forests and the Lauraceae having important ecological roles due to their widespread distribution and predominance in many plant communities [4,20]. In this type of ecosystem, water balance, depending on precipitation, temperature, and relative humidity, is generally viewed as a key factor with impacts on functional diversity, species richness and tree growth [21]. Together with other environmental variables, water availability directly affects photosynthesis and carbon assimilation, required for tree-ring width increment [22–25]. Despite often not being included in dendroclimatological analyses, additional factors may also affect tree growth, including topography, soil nutrient availability, competition, herbivory/phytophagy and natural disturbance [4,26,27].

The climate of the Azores, one of the Macaronesian archipelagos, is oceanic temperate, with high relative humidity, mild summers and winters, low daily and annual thermal amplitude, and precipitation evenly distributed throughout the year, although scarcer in summer [28,29]. Meanwhile, a steep altitudinal gradient is clearly expressed in the Azorean natural vegetation belts, with different types of zonal woodlands, forests, and scrubland [1,2,30]. Submontane laurel forest was likely much more common in the past, but still represents one of the more common types of natural extant forests [1,2]. The Lauraceae are represented in the Azores by *Laurus azorica* (Seub.) Franco, the dominant species in submontane laurel forests, which is also present in four other zonal natural forest and woodland types [1,2,30].

Previous studies addressed tree-ring growth in the Lauraceae. In Macaronesia growth rings generally showed an abrupt transition between thin and thick cell walls, characterizing early and latewood, and, in some cases, a delimiting marginal parenchyma band [31,32]. In Tenerife, *Laurus novocanariensis* Rivas Mart., Lousã, Fern.Prieto, E.Díaz, J.C.Costa & C.Aguiar showed a diffuse porous wood structure, with the entire cross-section of the stem being functional in terms of water transport, thereby reducing tree susceptibility to conditions of transient water limitation [33]. For this species, García-López et al. [34] found synchronous annual tree-rings, robust tree-ring chronologies, and positive correlations with annual precipitation. Outside Macaronesia, Reis-Avila and Oliveira [31] identified growth ring boundaries delimited by radially flattened fibers with thickened cell walls in the wood of *Nectandra amazonum* Nees and *Ocotea porosa* (Nees & Mart.) Barroso. Granato-Souza et al. [35] found that *Nectandra oppositifolia* Nees & Mart trees responded synchronously but negatively to high temperatures in the summer of the previous year and to high precipitation in the current year growing season. Moreover, previous research has also determined that several Lauraceae exhibit synchronous and climate-sensitive growth dynamics, and are therefore appropriate for dendrochronological analyses [31,33–35], raising the same possibility for *L. azorica*.

The Azorean natural forests provide critical ecosystem services, including habitat provisioning for biodiversity and carbon storage [30], but also protection against soil erosion and enhanced capabilities of water interception and infiltration [30,36–38]. However, no estimates of annual tree growth are available, impeding more precise estimations of annual carbon sequestration. Only a few studies have recently addressed dendrochronological topics devoted to Azorean trees [10,11,39–42], both introduced—*Pittosporum undulatum* Vent. (Pittosporaceae), *Pinus pinaster* Aiton (Pinaceae)—and native—*Juniperus brevifolia* (Seub.) Antoine (Cupressaceae), *Ilex azorica* Gand. (Aquifoliaceae) [43]. Câmara [44] estimated tree ages in two stands of laurel forest within a protected area, and Rego et al. [45] analyzed growth rings in a laurel forest invaded by *Clethra arborea* Aiton (Clethraceae). More recently, Matos et al. [14] described the growth ring anatomy and the relationship between dendrometric traits and the number of growth rings in *L. azorica*, confirming the diffuse porous structure of the wood, with solitary or randomly clustered distributed vessels, oriented perpendicularly to the distinct ring boundaries [14,46]. This suggests a water transport efficiency similar to that reported for *L. novocanariensis* [33], despite the

low risk of cavitation in the Azores, due to high water availability, except during the driest summer months at low-elevation sites.

Given the structural importance of the Lauraceae in Macaronesia [31–34], the need to enhance estimations of annual carbon sequestration, and the absence of climate–growth relationship studies for that family in the Azores, our research aimed to use dendroecological approaches to determine the basic climate–growth relationships in *Laurus azorica*. We compiled a large dataset of annually resolved ring width measurements derived from core samples collected from 203 trees in disjunct forest stands. We used a sequential combination of Random Forest and Generalized Linear Models to determine the relationships between radial growth and potential climate drivers. Thus, the main objective of the study was to investigate the limiting climatic factors affecting the radial growth of *L. azorica*. We addressed the following hypotheses: (1) based on a previous study, *L. azorica* will show distinctive tree-ring boundaries that will allow an accurate climate–growth relationship assessment; (2) the effect of previous year climate variables will be relevant because ring-porous broadleaved species are known to build their early wood before the onset of the growing season, from carbohydrates stored from the previous growing season (e.g., [47,48]); and (3) given the high relative humidity and annual precipitation of the archipelago [28,29], temperature will be the main limiting factor that affects tree growth, as previously shown for other Lauraceae species (e.g., [31]) and other studies in the Azores (e.g., [14,43]).

2. Materials and Methods

2.1. Study Area

The Azores is a Portuguese archipelago, located in the North Atlantic Ocean (36°55′–39°43′ N and 25°00′–31°15′ W) within a complex tectonic setting, near the triple junction between the Eurasian, Nubian, and North American plates [49]. Included in Macaronesia, it comprises nine volcanic islands (Figure 1) with a total land surface of 2323 km² [50]. The age of islands varies from 0.186 My for Pico island [51] to 6.01 My for Santa Maria island [52]. The climate in the archipelago is predominantly temperate (type C), namely Cfb (temperate with no dry season and with a mild summer), according to the Köppen–Geiger climate classification system (data from 1971 to 2000 [29]). Depending on the climatic conditions, particularly wind, water balance, and radiation, Azorean forests are distributed along eight vegetation belts, where plant species dominance and co-dominance change with altitude (see Elias et al. [1] for a full description). Despite the considerable changes that occurred in the Azorean land use in the 1950s, with subsequent replacement of the natural forests by crops and pastureland [53], the zonal vegetation is nowadays distributed as a continuum, with some niche partitioning between dominant species [2].

In this study, we limited sampling to *Laurus submontane* forest stands [1] occurring on two islands—São Miguel and Terceira—where the target species is dominant. A total of six stands were selected, allowing sampling across an altitudinal gradient to capture a wide range of environmental and climatic conditions (Figure 1): four stands at São Miguel Island—Pinhal da Paz (PP), Lombadas (LO), Povoação (PO) and Nordeste (NO)—and two at Terceira Island—Caldeira do Guilherme Moniz (GM) and Matela (MT). Selected stands were dominated by *Laurus azorica*, although mixed with several Azorean native trees, namely *Picconia azorica* (Tutin) Knobl (Oleaceae) and *Morella faya* Aiton (Wilbur) (Myricaceae) at the lower altitudes, and *Juniperus brevifolia* and *Ilex azorica* at higher altitudes. Invasive species were also present, including *Pittosporum undulatum*, *Clethra arborea* and *Hedychium gardnerianum* Sheppard ex Ker Gawl (Zingiberaceae) [1,30].

Selected forest stands differed slightly in terms of species composition and soil characteristics.

Caldeira do Guilherme Moniz (GM)—A stand located at a medium-elevation site (455 m), with annual mean temperature of 15.8 °C, annual precipitation of 1471 mm, almost flat terrain, and a vitric andosol containing more than 60% of unweathered pyroclastic material [54]. A large *L. azorica* population with young and old trees that occur spontaneously in a well preserved *Laurus submontane* forest with other native tree species, such as *Morella faya*, *Erica azorica* Hochst. ex Seub. (Ericaceae), *Ilex azorica*, and many native

fern species such as *Woodwardia radicans* (L.) Sm. (Blechnaceae), *Culcita macrocarpa* C.Presl. (Culcitaceae), and *Dryopteris* spp. (Dryopteridaceae).

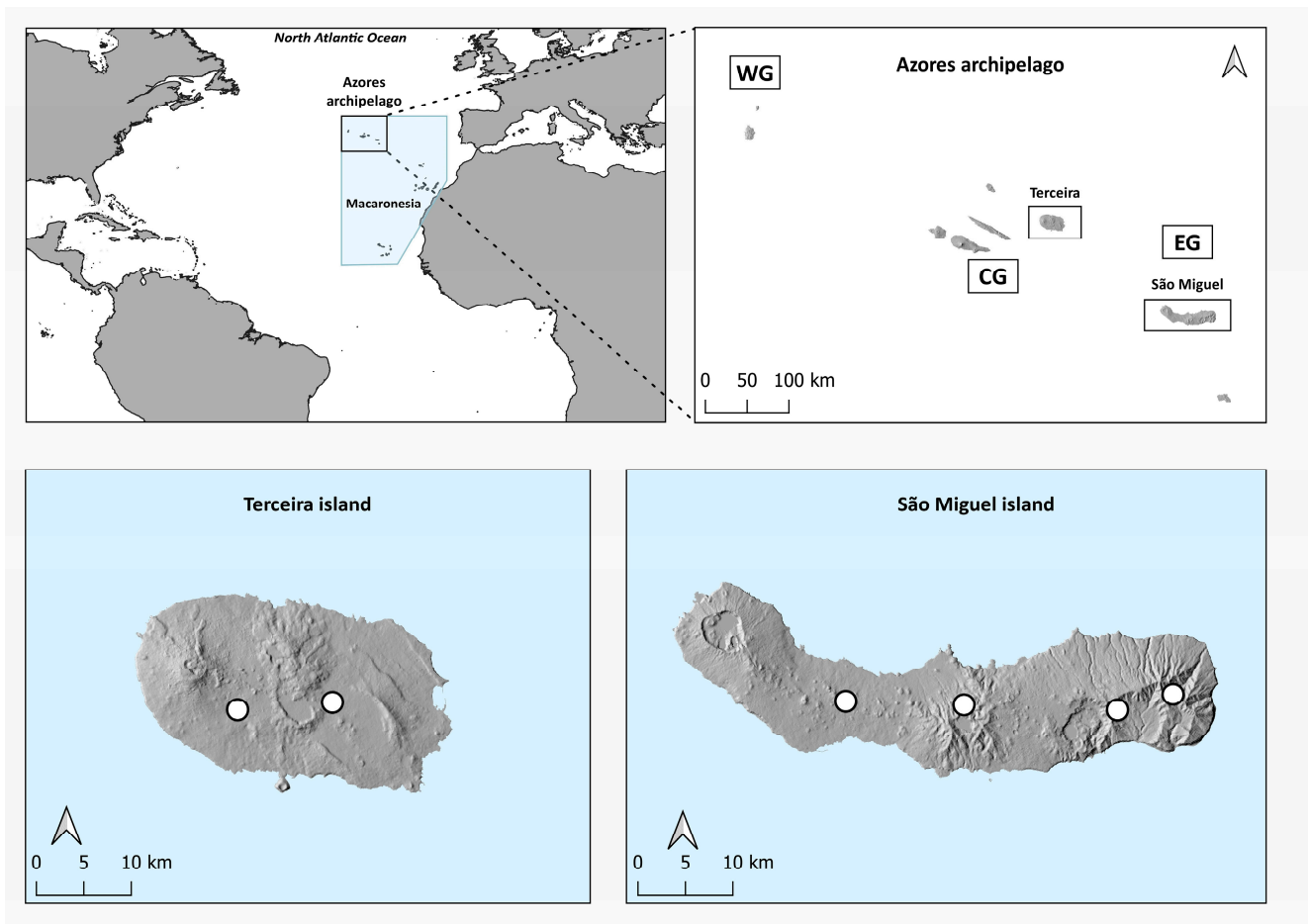


Figure 1. Map of the Azores archipelago (WG—Western Group, CG—Central Group, and EG—Eastern Group), framed on the North Atlantic Ocean and, more specifically, in Macaronesia. Both islands included in the study (Terceira and São Miguel) are highlighted, and circles indicate *Laurus azorica* sampled sites.

Matela (MT)—A stand located at a medium-elevation site (400 m), with annual mean temperature of 16.2 °C, annual precipitation of 1327 mm, almost flat terrain, and a ferruginous andosol, composed of trachytic pyroclastic material with a thin ferruginous layer [54]. A small *L. azorica* population with young and old trees that occur spontaneously in the remaining mosaics of natural vegetation with *Morella faya* and *Juniperus brevifolia*.

Pinhal da Paz (PP)—A stand located at a relatively low-elevation site (320 m), with annual mean temperature of 16.4 °C, annual precipitation of 1330 mm, somewhat rocky terrain, and a shallow allophanic regosol [55]. A small population of relatively young *L. azorica* trees that occur spontaneously in a forest recreation park with *Cryptomeria japonica* (Thunb. ex L.f.) D.Don (Cupressaceae) and other introduced species, such as *Pittosporum undulatum*. *Laurus azorica* trees were essentially located at a smooth hillside partly invaded by *Hedychium gardnerianum*.

Lombadas (LO)—A stand located at a relatively high-elevation site (600 m), with annual mean temperature of 15.2 °C, annual precipitation of 1459 mm, steep terrain (20–30° slope), and an unsaturated ferruginous andosol [55]. A large *L. azorica* population with young and old trees that occur spontaneously, in the remaining natural vegetation pockets, representing a transition between a *Laurus* submontane forest and a *Juniperus-Ilex* woodland, with *Morella faya*, *Erica azorica*, *Viburnum treleasei* Gand. (Adoxaceae), *Ilex azorica*,

Juniperus brevifolia, and many native fern species such as *Woodwardia radicans* and *Culcita macrocarpa*. *Cryptomeria japonica* stands occur nearby as well as some invasion by *Pittosporum undulatum* and *Hedychium gardnerianum*.

Povoação (PO)—A stand located at a medium-elevation site (470 m), with annual mean temperature of 15.3 °C, annual precipitation of 1352 mm, slightly sloped terrain (10° slope), and an allophanic ferruginous regosol [55]. A small *L. azorica* population with relatively old trees that occur spontaneously in a valley, with small patches of natural vegetation, representing *Laurus* submontane forest, with other native trees, such as *Morella faya* and *Erica azorica*, and some native ferns, such as *Woodwardia radicans* and *Culcita macrocarpa*. *Cryptomeria japonica* stands occur nearby as well as some invasion by *Pittosporum undulatum* and *Hedychium gardnerianum*.

Nordeste (NO)—A stand located at a relatively high-elevation site (590 m), with annual mean temperature of 15.1 °C, annual precipitation of 1434 mm, moderately steep terrain (10–20° slope), and a shallow allophanic ferruginous regosol [55]. A large *L. azorica* population with young and old trees that occur spontaneously in a mountain area, a large cover of natural vegetation, corresponding to a *Laurus* submontane forest, in some cases in a transition to a *Juniperus-Ilex* woodland, with *Morella faya*, *Erica azorica*, *Viburnum treleasei*, *Ilex azorica*, *Juniperus brevifolia*, and many native fern species such as *Woodwardia radicans*, *Culcita macrocarpa*, and *Dryopteris* spp. *Cryptomeria japonica* stands also occur nearby as well as some invasion by *Pittosporum undulatum*, *Clethra arborea*, and *Hedychium gardnerianum*.

2.2. Target Species—*Laurus azorica*

Distributed in tropical and subtropical climates, Lauraceae is a large family of tree taxa, including approximately 45 genera and 2850 species [56]. This family has an important ecological role in Macaronesia as one of the plant families structuring the laurel forest ecosystems in the Azores, Madeira, and on the Canary Islands [20], also contributing to the species richness of this biome [57]. Regarding its economic value, this family offers a wide range of applications, including high-quality timber and non-timber resources as spices and essential oils [58]. Individuals of the Azorean endemic *Laurus azorica* are recognized by a vertical trunk branching usually at a short distance from the base, with alternate glabrous leaves, but with hairy young leaves and shoots (Figure 2). According to the IUCN (International Union for Conservation of Nature) red list category and criteria, *L. azorica* is currently classified as a species of “Least Concern”, with the population trend being stable even though available habitats are severely fragmented [59]. In the archipelago, this species is present in four zonal vegetation types [1], mainly in *Laurus* submontane forests (300–600 m), but also in lowland laurel forests and montane woodlands. It can also be found in lava flows, coastal and mountain scrubland, and forested wetlands [60].

2.3. Sample Collection and Data Preparation

Field work was performed mainly in summer, between 2018 and 2022. Two to four wood cores were sampled per tree, resulting in 206 trees and 415 samples. At least 30 individual trees (large, adult trees were prioritized) were randomly sampled at each site, avoiding trees with any evidence of trunk, stem, or canopy damage. Wood cores were collected using a 5 mm diameter Pressler borer and kept in paper straws to prevent damage. Dendrometric traits, including diameter at breast height (dbh) and tree height, were measured.

In the laboratory, we followed standard dendrochronological techniques [11,61]. Increment core samples were air dried, mounted, and glued into wood supports. Cores were then sanded with progressively finer grades of abrasive paper (up to grid 600) until a proper polished surface was obtained. Ready-to-measure images of wood increment cores were taken using a LEICA S9I Stereozoom stereomicroscope with an incorporated 10 M.P. camera (Leica Microsystems Inc., Buffalo Grove, IL, USA), keeping a 50% overlap of sequential images to enable reliable stitching, which was performed with the open-source software Fiji—ImageJ [62].



Figure 2. *Laurus azorica* forest in São Miguel Island, Azores.

2.4. Tree-Ring Data Collection and Analysis

Measurements of annual tree-ring widths (TRW) were performed using Cybis CooRecorder (v. 9.3.1) to an accuracy of 0.01 mm. After converting measurements into .rwl files on Cybis CDendro (v. 9.3.1), visual cross-dating was performed on the PAST5 (SCIEM) software. To ensure the quality of the alignments on the cross-dating procedure, GLK (Gleichläufigkeit) [63,64], *T*-test, and Pearson's correlation coefficient statistics were used. Samples that could not be satisfactorily cross-dated were eliminated from further analysis.

The detrending procedure was applied to each individual tree-ring series using the package “dplr” for R software [65]. The procedure consisted of fitting a cubic smoothing spline with a 50% frequency response cut-off at 25 years to each individual ring width series [66–68]:

$$y_t = \beta_0 + \sum_{j=1}^p f_j(x_{tj})\beta_j + \varepsilon \quad (1)$$

where x_{tj} is the raw time series, f_j is the smoothing spline function (i.e., a degree 3 polynomial), β represents the regression coefficients, and ε represents the residuals. The response period was chosen given the length of the shorter chronology, which allows a more flexible approach. Subsequently, tree-ring indices (TRWi) were pre-whitened to remove short-term persistence (related to biological carry-over effect of trees) from tree-ring series. More-

over, 25% of the individual chronologies with the lowest correlation coefficients (within the site chronology) were removed to enhance the signal of the mean site chronologies. A TRWi chronology for each study site was built, averaging residual tree-ring series, to preserve climatic information while reducing the effect of autocorrelation [69,70], and using Tukey's biweight robust mean to reduce the influence of outliers [70–72]. Throughout the chronology building process, 131 samples were removed from further analysis.

Different measures were used to ensure chronology quality. Firstly, we used mean inter-series correlation (r_{bar}), as described in Wigley et al. [73], as a measure of the strength of the common growth "signal" within the chronologies. Secondly, we used subsample signal strength (SSS) to evaluate the loss of explanatory power due to a decreasing sample size back in time, calculated as:

$$SSS = (n \times (1 + (N - 1) \times r_{bar})) / (N \times (1 + (n - 1) \times r_{bar})), \quad (2)$$

where n and N are the number of cores or trees in the subsample and sample, respectively, and r_{bar} is the mean inter-series correlation. Only the portion of each chronology with $SSS \geq 0.85$ was used in modeling [74]. Thirdly, we used autocorrelation (AC1) to retrieve the carry-over effects of previous years, calculated using the $acf()$ function in R. Finally, we used a bootstrap procedure to estimate the standard deviation (SD) of each stand-level mean chronology ($N = 6$). Specifically, for each stand, a total of 1000 replicate mean chronologies were generated based on a random selection of 75% of the available individual tree chronologies. A corresponding SD (for each stand) was then computed from the 1000 replicates (Figure S1). This was used to further evaluate the consistency of the mean chronologies (e.g., [11]).

2.5. Dendroclimatic Models

2.5.1. Climatic Variables

Exact coordinates (centroid of each forest stand) obtained from sample sites were used to download minimum, maximum, and mean monthly temperature and monthly precipitation from the CHELSA timeseries dataset [75,76] with a spatial resolution of 30 arc seconds (ca. 1 km²). Different combinations of explanatory climatic variables were used for modeling (Table 1). In the case of seasonal values, we considered winter (December–February), spring (March–May), summer (June–August), and autumn (September–October), based on climate studies for the archipelago [28,29]. A detailed description of the climate at our study sites, based on the CHELSA database [75,76], is summarized and graphically represented in Figure S2.

2.5.2. Modeling Approaches

The relationship between TRWi and climatic variables was modeled by applying a sequential combination of Random Forest (RF)—which belongs to the group of machine learning algorithms—and Generalized Linear Models (GLMs), two methods that have been successfully used in growth ring analyses (e.g., [77–80]). A diagram with the analysis flow is presented in Figure 3.

RF is a flexible modeling tool that can accommodate binary, categorical, and high-dimensional data, while providing measures of predictor variable importance [81,82]. In this study, this method was used to determine climatic variable importance as a first step of climate–growth ring analysis [77,78,83,84]. Furthermore, RF models are nonparametric and can, therefore, consider nonlinear relationships and interactions between variables. RF is often used as an exploratory tool, as this method can identify relationships and interactions between variables without specifying their form a priori [85].

Afterwards, we incorporated the most important climatic terms (as selected by RF) in Generalized Linear Models to estimate the strength and direction of their effects on annual radial increment (i.e., tree-ring width, TRWi):

$$y_t = \beta_0 + \beta X_t + \varepsilon \quad (3)$$

where y_t is the response variable (TRWi), β_0 is the intercept (model constant), βX_t is a vector of regression coefficients and independent climatic variables, and ε represents the residuals.

To summarize, RF was used as a pre-step to calculate variable importance and reduce the number of potential predictor variables to be used in GLMs, while the latter were used to retrieve the direction of the effect of the selected variables.

Table 1. List of climatic variables used in models to explain the climate–growth relationships in six *Laurus azorica* forest stands in two Azores islands—Terceira and São Miguel.

Climate Variable	Year	Variable
Temperature	Current	Mean annual temperature
		Mean annual minimum temperature
		Mean annual maximum temperature
		Mean winter temperature
		Mean spring temperature
		Mean summer temperature
		Mean autumn temperature
		Mean winter minimum temperature
		Mean spring minimum temperature
	Mean summer minimum temperature	
	Mean autumn minimum temperature	
	Mean winter maximum temperature	
	Mean spring maximum temperature	
	Mean summer maximum temperature	
	Mean autumn maximum temperature	
	Monthly mean temperature	
	Monthly minimum temperature	
	Monthly maximum temperature	
Precipitation	Previous	Mean annual temperature
		Mean annual minimum temperature
		Mean annual maximum temperature
	Current	Monthly mean temperature
		Monthly minimum temperature
		Monthly maximum temperature
Previous	Annual precipitation	
	Winter precipitation	
	Spring precipitation	
Current	Summer precipitation	
	Autumn precipitation	
	Monthly precipitation	
Previous	Annual precipitation	
	Monthly precipitation	

2.5.3. Model Implementation and Variable Selection

Globally, we calculated 77 models, with 11 different models for the composite and each of the individual site chronologies (Table 2): nine different models in the first step of the RF, one optimal model in the second step of RF, and one reduced GLM.

RF models were calculated both for the whole dataset (composite chronology—CC, where we included the six growth ring chronologies) and for each individual site chronology. We used the *randomForest()* function from package “randomForest” for R software [81], with 10,000 trees per run, with an optimal value for the *mtry* parameter (with respect to out-of-bag error estimate—[81]) that was calculated for each model using the *tuneRF()* function.

In the first RF step, we calculated a saturated model, including all the available climatic variables from the present and the previous year, and nine other models based on temperature and/or precipitation from the current and/or the previous years, both for the composite and the individual site chronologies (Table 2). After this step, we retained only those climatic variables with an importance value above 10%, which were used to feed the second RF step.

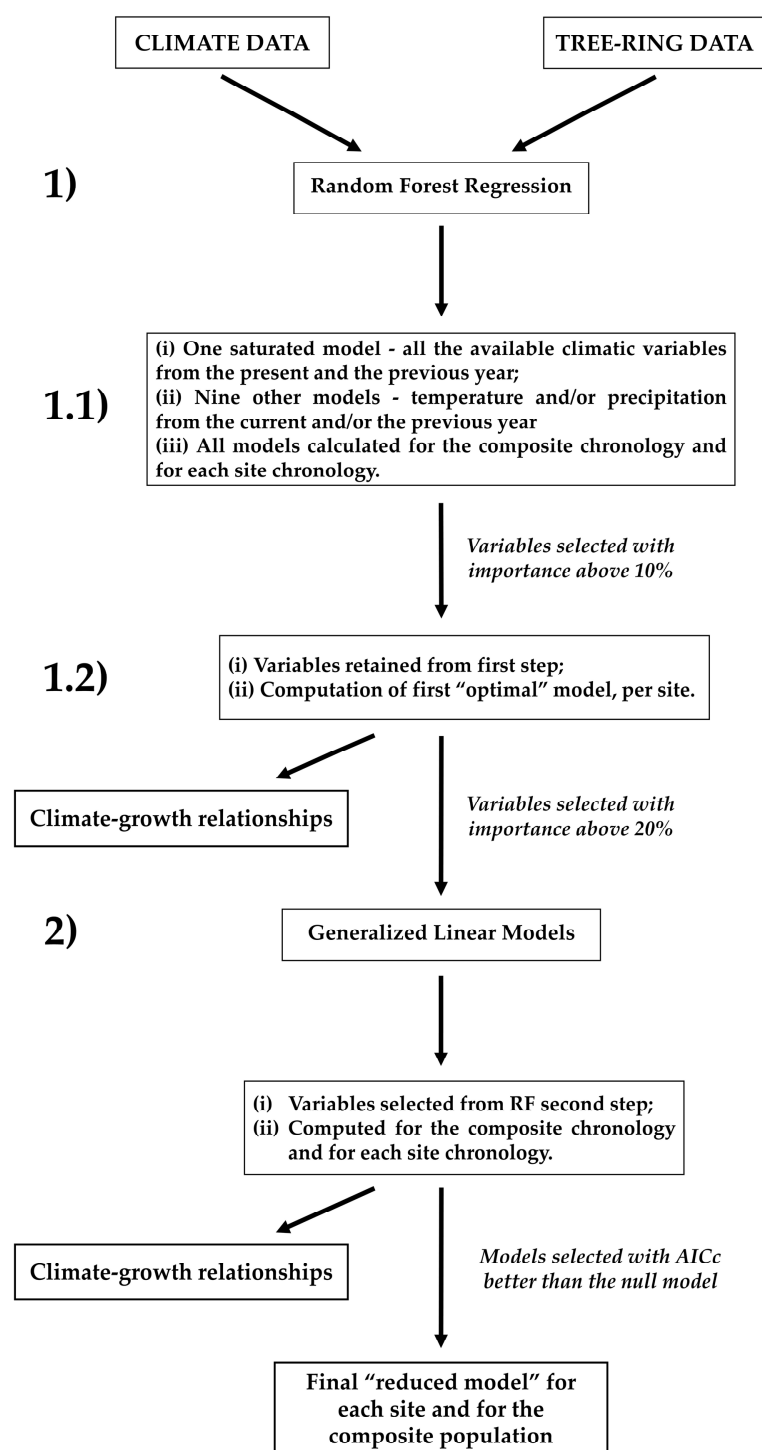


Figure 3. Flow diagram summarizing calculations of all dendroclimatic models used to explain the climate–growth relationships in six *Laurus azorica* forest stands in two Azores islands—Terceira and São Miguel. (1) RF modeling was used to inform the selection of the best explanatory climatic variables; (2) GLMs were used to estimate the direction and strength of the climatic variables on annual radial increment. *Italic* text indicates the selection parameters used at each step.

The second RF step allowed to build models (designated as “optimal”) including only those climatic variables with an importance value close to or above 20% (Table 2).

These climatic variables were used to feed the GLM analysis that was implemented using the *glm()* and *stepAIC()* functions in R, both for the composite and the individual site chronologies. To select the most parsimonious and informative GLMs we used the

following criteria (see [86–90]): (i) a corrected version (AICc) of Akaike Information Criterion (AIC) [91], to address possible overfitting due to low sample size; (ii) a comparison of that value with the AIC of the null model; (iii) adjusted R^2 , an estimate of model fit, calculated as the percentage of the sum of squares explained by the model [92]; and (iv) the significance of the regression coefficients ($p < 0.05$).

Table 2. List of all RF models and GLMs calculated to explain the climate–growth relationships in six *Laurus azorica* forest stands in two Azores islands—Terceira and São Miguel. The models included climatic data from the current year, from the previous year, or from both. The dependent variables corresponded to the composite or to the individual site chronologies.

Number	Model	Current	Previous	Both
Random Forest Step 1				
1	Saturated model (All variables)			x
2	Partially saturated model (All variables)	x		
3	Partially saturated model (All variables)		x	
4	Temperature model	x		
5	Temperature model		x	
6	Temperature model			x
7	Precipitation model	x		
8	Precipitation model		x	
9	Precipitation model			x
Random Forest Step 2				
10	Optimal model (Selected variables)	x	x	x
GLMs				
11	Reduced model (Selected variables)	x	x	x

3. Results

3.1. Site Chronologies

Chronology length varied from 48 years (1974 to 2019) in Lombadas—São Miguel to 67 years (1953 to 2020) in Povoação—São Miguel. First-order autocorrelation ranged from 0.20 to 0.53 and \bar{r} values ranged from 0.12 to 0.28. The complete assessment of the tree-ring series is summarized in Figure 4.

3.2. Climate–Growth Relationships

Based on computed SSS values for each site, climate–growth models were fitted for the period 1987 to 2018 (Figure 5).

Considering the results from the RF analyses (see Tables S1 and S2 for a full description), current and previous year temperatures were the main and most consistent drivers affecting radial growth (Table 3). Spring and early summer were the most important seasonal periods according to most models, particularly the composite model. The magnitude of the spring and early summer temperature effects varied by stand and ranged from positive to negative but was positive for the composite chronology. The second step of RF originated models with percentages of explained variance ranging from 16.92% to 48.38% (Table S3).

The GLM results also revealed a prominent effect of current or previous year temperatures for all chronologies (except for MT). Late spring and early summer temperature effects were detected in five of the six site chronologies (Tables 4 and S3). In the reduced models, possible precipitation effects were detected only in two cases: August precipitation with a positive effect on MT, and May precipitation with a negative effect on LO.

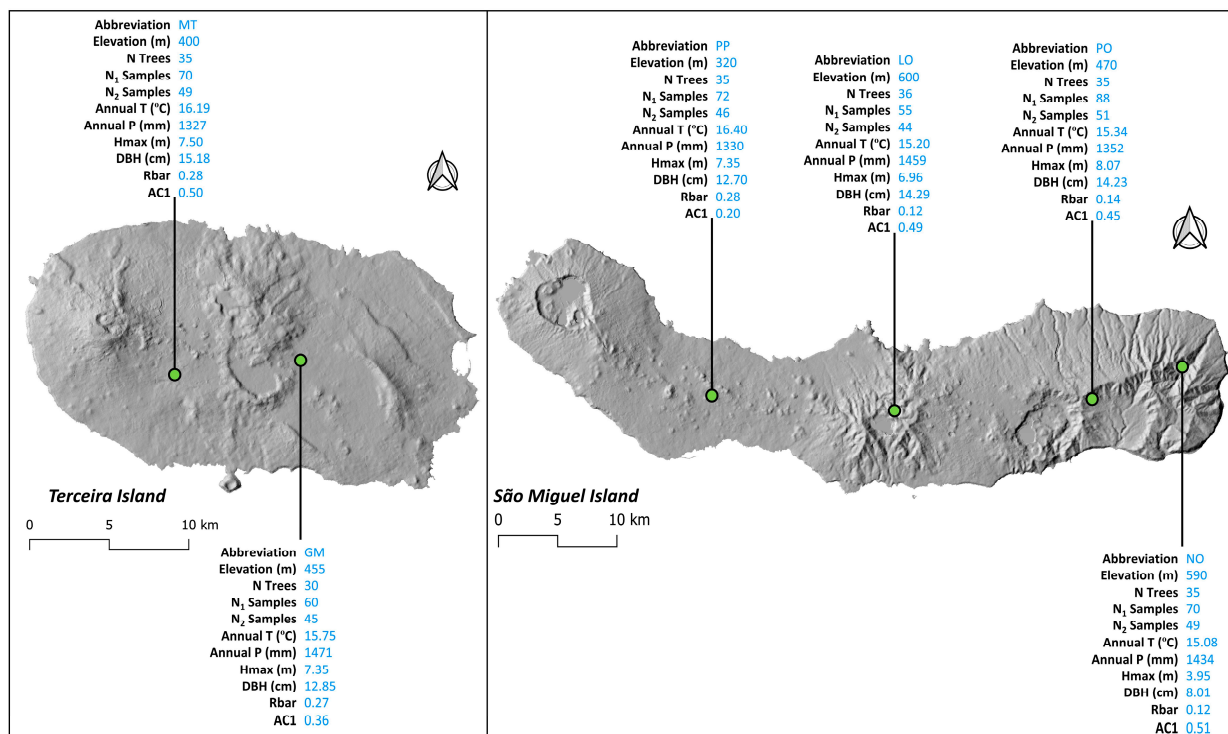


Figure 4. General characterization of the sampled sites at two Azores islands (Terceira and São Miguel), and basic parameters of the site chronologies used to study the climate–growth relationship in six *Laurus azorica* forest stands. Sampled sites are highlighted, including locality abbreviation, elevation (m), annual mean temperature (T), annual precipitation (P), number of trees (N Trees), total number of wood cores (N1), number of wood cores used in the dendroecological analysis (N2), average maximum tree height (Hmax), average diameter at breast height (DBH), mean inter-series correlation (Rbar), and the first-order autocorrelation (AC1).

Table 3. Modeling of climate–growth relationships in six *Laurus azorica* stands in two Azores islands, Terceira and São Miguel. Summary of the effects of the climatic variables retained in models both for the composite and for each individual site chronologies, after two steps of RF analysis. Direction of the effect (+ and -) was based on GLM results. Climatic variables were retained based on the respective importance value: above 10% in the first RF step; close to or above 20% in the second RF step.

ClimVar	CC	GM	MT	PP	LO	PO	NO	ClimVar	CC	GM	MT	PP	LO	PO	NO
T4		+						TminPre6				+			
T6			-		-			TminPre7						-	
T10		-						TminPre10						+	
Tmin3		+						TminPre12					+		
Tmin5	+			+				TmaxPre6	+	-					+
Tmin10	+			-				TmaxPre10						+	
Tmax3	-							P1			+				
Tmax5		-	-					P9						+	
Tmax6								Ppre4					+		
Tpre2							-	Ppre5					-		
Tpre6							+	Ppre8			+				
Tpre10			+					Ppre10						+	
TminPre2							-								

Note: + positive effect, - negative effect; T = temperature for different months (1–12); P = precipitation for different months (1–12); suffix Pre = previous year temperatures or previous year precipitation. CC, model for the composite chronology; GM to NO, models for each individual site chronology.

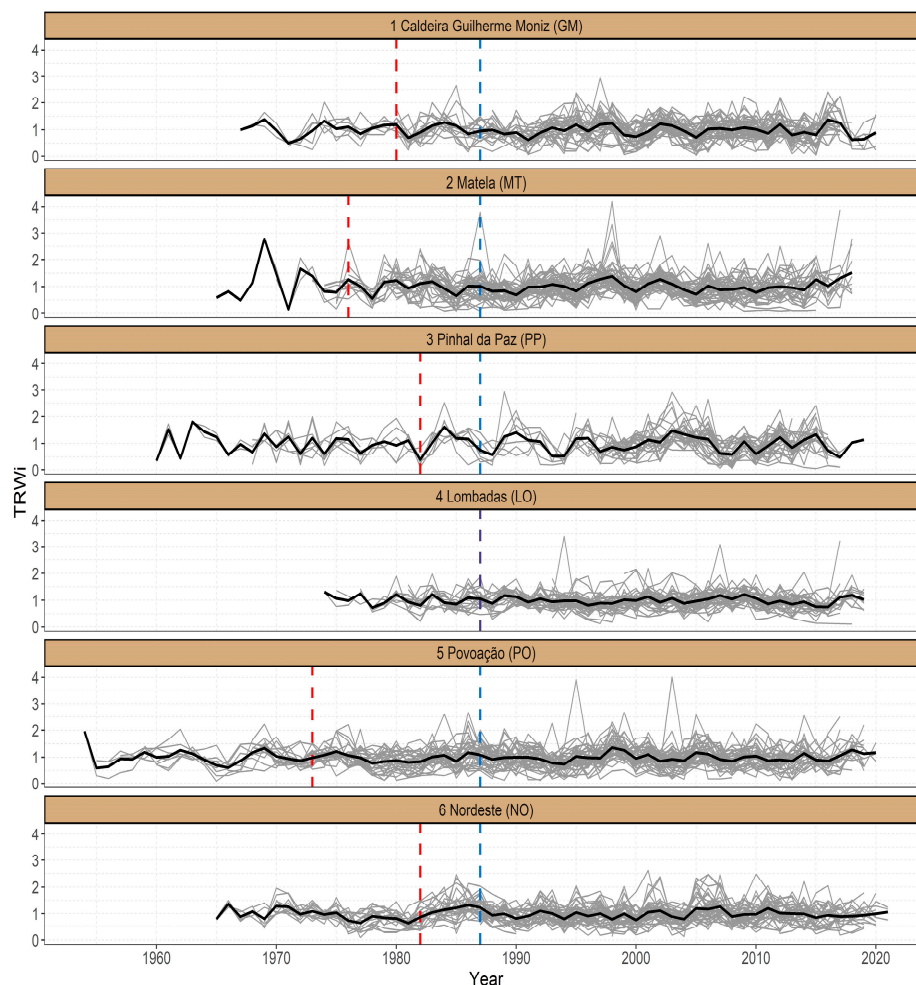


Figure 5. Spaghetti plots of *Laurus azorica* tree-ring indices for two populations at Terceira Island and four populations at São Miguel Island, Azores. Mean chronology—bold line; red dashed vertical lines—SSS ≥ 0.85 ; blue dashed vertical lines—cut-off used for modeling; LO site—purple dashed vertical line with SSS ≥ 0.85 and the cut-off used for modeling coinciding.

Table 4. Modeling of climate–growth relationships in six *Laurus azorica* stands in two Azores islands, Terceira and São Miguel. Performance of the reduced GLMs for the composite and for each individual chronology. Regression coefficients of each explanatory variable, AIC, AICc, null model AIC, and adjusted R².

Chronology	Model	Coefficients	AIC	AICc	Null Model AIC	R ²
CC	Tmin5 ***	+0.23618	317.02	317.234	349.084	0.171
	TmaxPre6 **	+0.11627				
GM	Tmax6 ***	−0.29387	15.592	17.074	27.623	0.386
	TmaxPre6 **	−0.22347				
MT	Ppre8 *	+0.002231	11.588	12.445	14.284	0.125
PP	Tmin5 ***	+0.6203	70.255	71.736	81.250	0.366
	TminPre6 *	+0.4827				
LO	T6 *	−0.0882183	−13.663	−12.182	−8.901	0.230
	Ppre5 *	−0.0008316				
PO	TminPre7 *	−0.14009	−7.3785	−5.897	7.716	0.442
	TminPre10 ***	+0.12668				
NO	Tpre6 *	+0.05826	−45.015	−43.534	−37.001	0.304
	TminPre2 **	−0.06556				

Note: + positive effect, − negative effect; * $p = 0.05$, ** $p = 0.01$, *** $p = 0.001$; T = temperature for different months (1–12); P = precipitation for different months (1–12); suffix Pre = previous year temperatures or previous year precipitation.

4. Discussion

4.1. Chronology Evaluation

We were able to reliably and accurately delineate and cross-date annual growth patterns in all *L. azorica* tree core samples. However, the relatively low r_{bar} values suggest that the growth of individual trees within each stand was not strongly synchronized. Similar results have also been reported for the Azorean endemic trees *Juniperus brevifolia* [11] and *Ilex azorica* [43], a common outcome in regions with low thermal amplitude and low seasonality (e.g., [93–96]). Stands at Terceira Island showed higher r_{bar} values than most of the sites at São Miguel Island, which suggests that other factors might be affecting or disturbing individual tree growth [27,97,98], including competition due to the presence of invasive plants that are more common in São Miguel natural forests [1,30].

Chronology length differed among stands due to the different ages of the forest stands, as natural forests have been deeply disturbed in the Azores, some being secondary and not primordial forests [1]. For example, most of the *Laurus* submontane forests have been replaced by pastureland, exotic woodland, or production forests [1]. Likewise, developed chronologies were relatively short, with a maximum of 67 years. Considerable changes have occurred in the Azorean soil cover, starting with human settlement and intensifying in the 1950s, which influenced the distribution and age of the extant natural forests [53].

4.2. Modeling Constraints

Our stepwise approach to RF allowed selecting a range of explanatory climatic variables corresponding to importance values above 20% and providing a reasonable percentage of explained variance comparing to previous studies (e.g., [99–101]). The GLM approach was also previously used in other studies from the Azores archipelago (e.g., [14,41,43]). Moreover, although delivering a useful estimation of the direction of the effect, the final GLMs did not show a relevant improvement in terms of model evaluation statistics (AICc and adjusted R^2) compared to the climatic variables selected in the second step of RF. A possible explanation is the fact that RF is a versatile, robust, and stable analysis. Apart from being a straightforward method in terms of the simplicity of its parameters, it generates low bias and moderate variance [102–104]. This error reduction is related to the random selection of the elements used for the induction of each tree, reducing the correlation between individual models, and providing predictions with greater stability [103,105]. RF models provided an indication of the importance of specific climatic variables for tree growth [77,78,83,84], while GLMs provided more explicit information describing the strength and direction of these effects. However, our GLM regression analyses only considered linear additive effects and were arguably sensitive to outliers [106,107], although showing consistency with RF results. Hence, the discussion of the modeling results will consider a global evaluation based on the two complementary approaches—RF and GLM.

4.3. Climate–Growth Relationships—Temperature Effect

The overall composite chronology (metapopulation) helped us to understand similarities among sampled stands and the overall effect of the climatic variables on *L. azorica* radial growth in the Azores. The models derived for the composite chronology showed that growth rings in *L. azorica* were predominantly sensitive to current and previous year spring temperatures. As a ring-porous species, *L. azorica* xylem vessels include distinct pits in tangential section, which allows water transport between individual vessels. Pit structure together with diffusely distributed xylem vessels may function to reduce tree susceptibility to environmental stressors, including drought [14,108]. Thus, this mechanism, together with warmer temperatures in late spring and early summer, may enhance photosynthetic performance for the rest of the growing season, potentiating carbon uptake and positively affecting tree growth (e.g., [108–110]). Nonetheless, the role of carbon storage in the previous year is still an open question that requires experimental studies (see [111,112]). Additionally, submontane and montane forests in the Azores are usually associated with high levels of occult or horizontal precipitation, intercepted by the vegeta-

tion cover [113,114]. This ensures water availability that, together with warm temperatures, may favor radial growth [115,116].

Further explanation for our results might be related to an earlier onset of cambial activity and cell differentiation during relatively warm spring conditions. In fact, the flowering season in *Laurus azorica* might start as early as November or December, extending until April, followed by a fruiting season that extends into summer and autumn [117]. Thus, warmer spring and early summer months might extend the length of the growing, flowering, and fruiting seasons, and, consequently, the length of the total period available for wood production in a given year [118].

An exception to this pattern, in some cases (composite, GM, MT and LO), was the negative effect of high summer temperatures, particularly of maximum temperature. This suggests that extremely high temperatures might affect tree growth due to water imbalance [115,116]. Despite the positive impulse associated with high temperatures at the beginning of the growing season, the subsequent negative effect of extremely high summer temperatures has been reported for other broadleaved species (e.g., [119,120]) and for the Azorean tree *Ilex azorica* [43]. Summer water stress has been shown to affect radial growth rate [121–123]. Indeed, extremely high summer temperatures increase evapotranspiration and reduce water availability, prompting stomatal closure. This will decrease photosynthetic activity, carbohydrate storage, and, consequently, reduce cambial activity [124–126]. Within the Lauraceae, extensive studies at Brazil Atlantic Forest with *Nectandra* spp. reported that warmer summers suppressed tree growth due to water stress and increased evapotranspiration [31,35,127].

4.4. Climate–Growth Relationships—Precipitation Effect

Globally, no relevant effect of precipitation was found, except in MT and PO, where a positive effect of late spring and summer precipitation was observed, related to the water balance required for tree growth during the drier months [128], as previously observed in other broadleaved species (e.g., [129–131]). In fact, the archipelago presents high relative humidity and a precipitation evenly distributed throughout the year, except during the driest summer months [28,29].

4.5. Climate–Growth Relationships—Previous Year Effect

We found an effect of climatic variables from the previous year on growth rings, which has been previously reported for diffuse porous species (e.g., [47,48]). Research in boreal, temperate, and tropical forests, with a broad range of tree taxa, has also reported relationships between tree growth and previous year climatic variables (e.g., [132–134]). This so-called legacy effect is controlled by several interactions between the environment and tree physiology [71]. It also suggests lagged physiological effects persevering longer than the current year [135–137]. For example, non-structural carbohydrate (NSC) allocation and storage might affect tree growth in the following years [135,138–142]. Warmer temperatures at the end of the growing season (as it happens in the Azores archipelago) can extend its length. Thereby, the NSC stock that will be available for the next growing season will be increased (e.g., [109,110]). However, NSC accumulation in *L. azorica* has not been investigated.

4.6. Climate–Growth Relationships—Differences among Sites

We obtained slightly different climate–growth relationships among sites that can be linked to different site conditions (i.e., elevation) existing in the archipelago (see [1,2]), possible competition with other native or exotic species (e.g., [26,143–145]), differences between the microclimates (e.g., [146,147]), and high variability within stands (low r_{bar} values).

Regarding stand characteristics (soil type, slope, and species composition), the most abundant soil types were ferruginous andosols (present in MT, LO, PO, and NO) and shallow allophanic regosols (present in PP, PO, and NO), except for GM, with a vitric andosol. Ferruginous andosols have low water infiltration capacity [55], which could

reduce water availability for trees at four of the studied stands. Sloped terrain was mostly found at São Miguel Island stands (PP, LO, PO, and NO), while species composition was relatively homogeneous in all stands, with the presence of exotic species and, consequently, possible competition. Despite some local variation, laurel forests in the Azores generally occur in similar environmental conditions, with a considerable amount of organic matter on soils, even for very shallow regosols (see [30]). In fact, no relevant environmental differences have been found between laurel forests on different Azores islands in previous studies, except for some local variation in plant community composition [1,30]. Therefore, the establishment of a direct link between differences in climate–growth relationships and stand characteristics is not possible at this stage.

Biotic factors also mediate growth responses to climate (e.g., [148,149]), even though our data transformations (i.e., detrending) should have removed most of these biotic effects. Nevertheless, it seems likely that there may be residual growth variance that is attributed to competition or age (e.g., [26,142,144]). Matos et al. [14] also found differences in radial growth rate between different stands of *L. azorica* at different elevations. Other studies addressing one tree species at different elevations also found distinct climate–growth relationships among sites (e.g., [150–152]). Moreover, different responses of tree growth to climate have also been found at the intra-individual scale (e.g., [153]). Furthermore, different populations could have become locally adapted or acclimated. Many studies show that both local adaptation and acclimation are quite common in plant species (e.g., [153,154]). However, experimental studies would be needed to confirm differentiation among *L. azorica* populations (e.g., [154–158]).

Our results emphasize the importance of modeling under different site conditions to better encompass the various situations and factors affecting growth ring width and its inherent variation.

5. Conclusions

Our study demonstrated the possibility of developing reliable tree-ring chronologies of a key species of the Azorean laurel forest ecosystems, showing that the relationship between tree-ring widths and climate parameters is mainly connected to temperature of the current and previous years. Hence, this work, together with recent studies dealing with other important laurel forest trees [11,43], contributes to building baseline climate–growth relationships in an island forest under low climatic seasonality. Furthermore, future dendrochronological studies could be applied to other relevant native or introduced species (e.g., [10,11]), or to other Macaronesian islands (e.g., [13,16–19,34]). Nonetheless, due to the high levels of within-stand variation, and to refine the climate–growth analysis, different approaches and proxies will have to be explored in the future, including early and latewood vessel area [159,160] since most native species are angiosperms. Moreover, other insights (e.g., site characteristics and physiological processes) could be tested in future works to refine the relation between climate and radial tree growth in the Azores archipelago.

Supplementary Materials: The following supporting information can be downloaded at: <https://www.mdpi.com/article/10.3390/f14020166/s1>, Figure S1: Bootstrapped mean chronology for all studied sites. Years on x axis and tree-ring indices (TRWi) on y axis; Figure S2: Average temperatures (lines) and monthly precipitation (bars) for all study sites. Data were extracted from CHELSA timeseries dataset with a spatial resolution of 30-degree seconds; Table S1: Results from the first RF step (various combinations of climatic variables, i.e., temperature and precipitation from current and/or previous year) for composite and site chronologies, with the respective variable importance (%IncMSE). Those variables that were selected for the second step of RF are marked in green; Table S2: Results from second RF step (based on the variables selected on the first RF step), for composite and site chronologies, with the respective variable importance (%IncMSE) and increase in node purity (IncNodePurity). Those variables that were selected for the GLM analysis are marked in green; Table S3: Performance of all RF and GLM tested models (based on the variables selected on the second RF step) for composite and site chronologies, with the respective regression coefficients

for each explanatory variable, AIC, AICc, null model AIC, adjusted R^2 , mean of squared residuals, and % of explained variance.

Author Contributions: Conceptualization: D.C.P., L.S.; Data curation: D.C.P.; Formal analysis: D.C.P., J.J., L.S.; Methodology: D.C.P., J.J., L.S.; Field work: D.C.P., R.B.E., L.S.; Supervision: L.B.S., R.B.E., L.S.; Writing—original draft: D.C.P.; Writing—review and editing: D.C.P., J.J., L.B.S., R.B.E., L.S. All authors have read and agreed to the published version of the manuscript.

Funding: D.C.P. is currently supported by a PhD studentship grant (SFRH/BD/136336/2018) from the Foundation for Science and Technology (FCT) of the Ministry of Science, Technology, and Higher Education. This research was also supported by national funds through the FCT under (FCT) UIDB/50027/2020 (CIBIO). J.J. was supported by the Alexander von Humboldt postdoctoral fellowship and the Slovenian Research Agency (“Forest Biology, Ecology and Technology—P4-0107”).

Institutional Review Board Statement: Not applicable.

Informed Consent Statement: Not applicable.

Data Availability Statement: The data presented in this study are available on request from the corresponding author.

Acknowledgments: The authors would like to thank the technician Roberto Resendes for the field assistance during sampling.

Conflicts of Interest: The authors declare no conflict of interest. The funders had no role in the design of the study; in the collection, analyses, or interpretation of data; in the writing of the manuscript; or in the decision to publish the results.

References

- Elias, R.B.; Gil, A.; Silva, L.; Fernández-Palacios, J.M.; Azevedo, E.B.; Reis, F. Natural Zonal Vegetation of the Azores Islands: Characterization and Potential Distribution. *Phytocoenologia* **2016**, *46*, 107–123. [[CrossRef](#)]
- Pavão, D.C.; Elias, R.B.; Silva, L. Comparison of Discrete and Continuum Community Models: Insights from Numerical Ecology and Bayesian Methods Applied to Azorean Plant Communities. *Ecol. Modell.* **2019**, *402*, 93–106. [[CrossRef](#)]
- Mueller-Dombois, D.; Boehmer, H.J. Origin of the Hawaiian Rainforest and Its Transition States in Long-Term Primary Succession. *Biogeosciences* **2013**, *10*, 5171–5182. [[CrossRef](#)]
- Hanz, D.M.; Cutts, V.; Barajas-Barbosa, M.P.; Algar, A.C.; Beierkuhnlein, C.; Fernández-Palacios, J.M.; Field, R.; Kreft, H.; Steinbauer, M.J.; Weigelt, P.; et al. Climatic and Biogeographical Drivers of Functional Diversity in the Flora of the Canary Islands. *Glob. Ecol. Biogeogr.* **2022**, *31*, 1313–1331. [[CrossRef](#)]
- Kier, G.; Kreft, H.; Tien, M.L.; Jetz, W.; Ibsch, P.L.; Nowicki, C.; Mutke, J.; Barthlott, W. A Global Assessment of Endemism and Species Richness across Island and Mainland Regions. *Proc. Natl. Acad. Sci. USA* **2009**, *106*, 9322–9327. [[CrossRef](#)]
- Weigelt, P.; Jetz, W.; Kreft, H. Bioclimatic and Physical Characterization of the World’s Islands. *Proc. Natl. Acad. Sci. USA* **2013**, *110*, 15307–15312. [[CrossRef](#)]
- Zimowski, M.; Leuschner, H.H.; Gärtner, H.; Bergmeier, E. Age and Diversity of Mediterranean Dwarf Shrublands: A Dendrochronological Approach along an Altitudinal Gradient on Crete. *J. Veg. Sci.* **2014**, *25*, 122–134. [[CrossRef](#)]
- Battipaglia, G.; De Micco, V.; Brand, W.A.; Linke, P.; Aronne, G.; Saurer, M.; Cherubini, P. Variations of Vessel Diameter and $\Delta 13C$ in False Rings of *Arbutus unedo* L. Reflect Different Environmental Conditions. *New Phytol.* **2010**, *188*, 1099–1112. [[CrossRef](#)]
- Copenheaver, C.A.; Gärtner, H.; Schäfer, I.; Vaccari, F.P.; Cherubini, P. Drought-Triggered False Ring Formation in a Mediterranean Shrub. *Botany* **2010**, *88*, 545–555. [[CrossRef](#)]
- Vieira, J.; Campelo, F.; Nabais, C. Dendrochronology of Maritime Pine in the Middle of the Atlantic Ocean. *Dendrochronologia* **2017**, *45*, 73–80. [[CrossRef](#)]
- Pavão, D.; Jevšenak, J.; Petrillo, M.; Camarinho, R.; Rodrigues, A.; Silva, L.B.; Elias, R.B.; Silva, L. Dendrochronological Potential of the Azorean Endemic Gymnosperm *Juniperus brevifolia* (Seub.) Antoine. *Dendrochronologia* **2022**, *71*, 125901. [[CrossRef](#)]
- Christopoulou, A.; Gmińska-Nowak, B.; Özarlan, Y.; Wążny, T. Aegean Trees and Timbers: Dendrochronological Survey of the Island of Symi. *Forests* **2020**, *11*, 1266. [[CrossRef](#)]
- Fernández de Castro, A.G.; Rozas, V.; Fuertes-Aguilar, J.; Moreno-Saiz, J.C. Demographic and Dendrochronological Evidence Reveals Highly Endangered Status of a Paleoendemic Woody Mallow from the Canary Islands. *Biodivers. Conserv.* **2020**, *29*, 469–485. [[CrossRef](#)]
- Matos, B.; Silva, L.B.; Camarinho, R.; Rodrigues, A.S.; Rego, R.; Câmara, M.; Silva, L. Linking Dendrometry and Dendrochronology in the Dominant Azorean Tree *Laurus azorica* (Seub.) Franco. *Forests* **2019**, *10*, 538. [[CrossRef](#)]
- Génova, M.; Ortega, P.; Sadornil, E. The Effects of Fire on *Pinus sylvestris* L. as Determined by Dendroecological Analysis (Sierra de Gredos, Spain). *IForest* **2022**, *15*, 171–178. [[CrossRef](#)]

16. Jonsson, S.; Gunnarson, B.; Criado, C. Drought Is the Major Limiting Factor for Tree-Ring Growth of High-Altitude Canary Island Pines on Tenerife. *Geogr. Ann. Ser. A Phys. Geogr.* **2002**, *84*, 51–71. [[CrossRef](#)]
17. Pérez-De-Lis, G.; García-González, I.; Rozas, V.; Arévalo, J.R. Effects of Thinning Intensity on Radial Growth Patterns and Temperature Sensitivity in *Pinus canariensis* Afforestations on Tenerife Island, Spain. *Ann. For. Sci.* **2011**, *68*, 1093–1104. [[CrossRef](#)]
18. Rozas, V.; García-González, I.; Pérez-De-Lis, G.; Arévalo, J.R. Local and Large-Scale Climatic Factors Controlling Tree-Ring Growth of *Pinus Canariensis* on an Oceanic Island. *Clim. Res.* **2013**, *56*, 197–207. [[CrossRef](#)]
19. Rozas, V.; Pérez-de-Lis, G.; García-González, I.; Arévalo, J.R. Contrasting Effects of Wildfire and Climate on Radial Growth of *Pinus canariensis* on Windward and Leeward Slopes on Tenerife, Canary Islands. *Trees–Struct. Funct.* **2011**, *25*, 895–905. [[CrossRef](#)]
20. Fernández-Palacios, J.M.; Arévalo, J.R.; Balguerías, E.; Barone, R.; de Nascimento, L.; Elias, R.B.; Delgado, J.D.; Fernández-Lugo, S.; Méndez, J.; Naranjo Cigala, A.; et al. La Laurisilva. In *Canarias, Madeira y Azores*; Macaronesia Editorial: Santa Cruz de Tenerife, Spain, 2017.
21. Vieira, J.; Carvalho, A.; Campelo, F. Tree Growth Under Climate Change: Evidence From Xylogensis Timings and Kinetics. *Front. Plant Sci.* **2020**, *11*, 90. [[CrossRef](#)]
22. Cuny, H.E.; Rathgeber, C.B.K.; Frank, D.; Fonti, P.; Fournier, M. Kinetics of Tracheid Development Explain Conifer Tree-Ring Structure. *New Phytol.* **2014**, *203*, 1231–1241. [[CrossRef](#)] [[PubMed](#)]
23. Giguère-Croteau, C.; Boucher, É.; Bergeron, Y.; Girardin, M.P.; Drobyshev, I.; Silva, L.C.R.; Hélie, J.F.; Garneau, M. North America’s Oldest Boreal Trees Are More Efficient Water Users Due to Increased [CO₂], but Do Not Grow Faster. *Proc. Natl. Acad. Sci. USA* **2019**, *116*, 2749–2754. [[CrossRef](#)] [[PubMed](#)]
24. Marchand, W.; Girardin, M.P.; Hartmann, H.; Depardieu, C.; Isabel, N.; Gauthier, S.; Boucher, É.; Bergeron, Y. Strong Overestimation of Water-Use Efficiency Responses to Rising CO₂ in Tree-Ring Studies. *Glob. Chang. Biol.* **2020**, *26*, 4538–4558. [[CrossRef](#)] [[PubMed](#)]
25. Baldocchi, D.; Penuelas, J. The Physics and Ecology of Mining Carbon Dioxide from the Atmosphere by Ecosystems. *Glob. Chang. Biol.* **2019**, *25*, 1191–1197. [[CrossRef](#)]
26. He, R.; Wang, X.; Liu, T.; Guo, L.; Wang, B.; Khan, A. Impact of Competition on the Growth of *Pinus tabulaeformis* in Response to Climate on the Loess Plateau of China. *Plant Ecol.* **2022**, *223*, 353–368. [[CrossRef](#)]
27. Luo, Y.; McIntire, E.J.B.; Boisvenue, C.; Nikiema, P.P.; Chen, H.Y.H. Climatic Change Only Stimulated Growth for Trees under Weak Competition in Central Boreal Forests. *J. Ecol.* **2020**, *108*, 36–46. [[CrossRef](#)]
28. Azevedo, E.M.V.B. Condicionantes Dinâmicas Do Clima Do Arquipélago Dos Açores. Elementos Para o Seu Estudo. *Açoreana* **2001**, *9*, 309–317.
29. Couto, M.A.G. *Atlas Climático de Los Archipiélagos de Canarias, Madeira y Azores Atlas Climático Dos Arquipélagos Das Canárias, Da Madeira e Dos Açores*; Aemet: Madrid, Spain, 2012; p. 79.
30. Borges Silva, L.C.; Pavão, D.C.; Elias, R.B.; Moura, M.; Ventura, M.A.; Silva, L. Taxonomic, Structural Diversity and Carbon Stocks in a Gradient of Island Forests. *Sci. Rep.* **2022**, *12*, 1–16. [[CrossRef](#)]
31. Reis-Avila, G.; Oliveira, J.M. Lauraceae: A Promising Family for the Advance of Neotropical Dendrochronology. *Dendrochronologia* **2017**, *44*, 103–116. [[CrossRef](#)]
32. Schweingruber, F.H.; Börner, A.; Schulze, E.-D. *Atlas of Stem Anatomy in Herbs, Shrubs and Trees—Volume 2*; Springer: Berlin/Heidelberg, Germany, 2013; ISBN 978-3-642320434-0.
33. Balabasquer, L.D.V. *Dendroecología de Laurus novocanariensis En Cinco Localidades de Tenerife, Islas Canarias*; Universidad de La Laguna: La Laguna, Spain, 2021.
34. García-López, M.A.; Rozas, V.; Olano, J.M.; Sangüesa-Barreda, G.; García-Hidalgo, M.; Gómez-González, S.; López-Rubio, R.; Fernández-Palacios, J.M.; García-González, I.; García-Cervigón, A.I. Tree-Ring Distinctness, Dating Potential and Climatic Sensitivity of Laurel Forest Tree Species in Tenerife Island. *Dendrochronologia* **2022**, *76*, 126011. [[CrossRef](#)]
35. Granato-Souza, D.; Adenisky-Filho, E.; Esemann-Quadros, K. Dendrochronology and Climatic Signals in the Wood of *Nectandra oppositifolia* from a Dense Rain Forest in Southern Brazil. *J. For. Res.* **2019**, *30*, 545–553. [[CrossRef](#)]
36. Malheiro, A. Geological Hazards in the Azores Archipelago: Volcanic Terrain Instability and Human Vulnerability. *J. Volcanol. Geotherm. Res.* **2006**, *156*, 158–171. [[CrossRef](#)]
37. Louvat, P.; Allègre, C.J. Riverine Erosion Rates on Sao Miguel Volcanic Island, Azores Archipelago. *USDA For. Serv.-Gen. Tech. Rep. RMRS-GTR* **1998**, *148*, 177–200. [[CrossRef](#)]
38. Fontes, J.C.; Pereira, L.S.; Smith, R.E. Runoff and Erosion in Volcanic Soils of Azores: Simulation with OPUS. *Catena* **2004**, *56*, 199–212. [[CrossRef](#)]
39. Wunder, J. *Technical Report: Age Estimation of *Pittosporum undulatum* from São Miguel, Azores, Portugal*; Wunder Consulting: Pfäffikon, Switzerland, 2010.
40. Teixeira, A.; Mir, C.; Borges Silva, L.; Hahndorf, I.; Silva, L. Invasive Woodland Resources in the Azores: Biomass Availability for 100% Renewable Energy Supply in Graciosa Island. In Proceedings of the 23rd European Biomass Conference and Exhibition, Vienna, Austria, 1–4 June 2015.
41. Borges Silva, L.; Teixeira, A.; Alves, M.; Elias, R.B.; Silva, L. Tree Age Determination in the Widespread Woody Plant Invader *Pittosporum undulatum*. *For. Ecol. Manag.* **2017**, *400*, 457–467. [[CrossRef](#)]
42. Borges Silva, L.; Lourenço, P.; Teixeira, A.; Azevedo, E.B.; Alves, M.; Elias, R.B.; Silva, L. Biomass Valorization in the Management of Woody Plant Invaders: The Case of *Pittosporum undulatum* in the Azores. *Biomass Bioenergy* **2018**, *109*, 155–165. [[CrossRef](#)]

43. Pavão, D.; Jevšenak, J.; Engblom, J.; Silva, L.B.; Elias, R.B.; Silva, L. Tree Growth-Climate Relationship in the Azorean Holly in a Temperate Humid Forest with Low Thermal Amplitude. *Dendrochronologia* **2023**, *77*, 126050. [[CrossRef](#)]
44. Câmara, M.I.M. *Tree Age Estimation in an Invaded Natural Forest in São Miguel Island, Azores*; Universidade dos Açores: Ponta Delgada, Portugal, 2016.
45. Rego, R.; Borges Silva, L.; Medeiros, F.; Porteiro, J.; Silva, L. Ecological Characterization as the First Step Towards the Conservation of Natural Unprotected Areas: A Case Study in the Azores. In Proceedings of the European Meeting of Phytosociology, Biogeography and Syntaxonomy of the Atlantic Regions, Praia, Cape Verde, 5–7 November 2017.
46. Schweingruber, F.H.; Börner, A.; Schulze, E.-D. *Atlas of Stem Anatomy in Herbs, Shrubs and Trees—Volume 1*; Springer: Berlin/Heidelberg, Germany, 2011; ISBN 9783642116377.
47. Buttó, V.; Millan, M.; Rossi, S.; Delagrangé, S. Contrasting Carbon Allocation Strategies of Ring-Porous and Diffuse-Porous Species Converge Toward Similar Growth Responses to Drought. *Front. Plant Sci.* **2021**, *12*, 2990. [[CrossRef](#)]
48. García González, I.; Eckstein, D. Climatic Signal of Earlywood Vessels of Oak on a Maritime Site. *Tree Physiol.* **2003**, *23*, 497–504. [[CrossRef](#)]
49. Miranda, J.M.; Luis, J.F.; Lourenço, N.; Goslin, J. Distributed Deformation Close to the Azores Triple “Point”. *Mar. Geol.* **2014**, *355*, 27–35. [[CrossRef](#)]
50. Forjaz, V.H.; Tavares, J.M.; Azevedo, E.M.V.B.; Nunes, J.C. *Atlas Básico Dos Açores*; Observatório Vulcanológico e Geotérmico dos Açores: Lagoa, Portugal, 2004.
51. Costa, A.C.G.; Hildenbrand, A.; Marques, F.O.; Sibrant, A.L.R.; Santos de Campos, A. Catastrophic Flank Collapses and Slumping in Pico Island during the Last 130 Kyr (Pico-Faial Ridge, Azores Triple Junction). *J. Volcanol. Geotherm. Res.* **2015**, *302*, 33–46. [[CrossRef](#)]
52. Ramalho, R.S.; Helffrich, G.; Madeira, J.; Cosca, M.; Thomas, C.; Quartau, R.; Hipólito, A.; Rovere, A.; Hearty, P.J.; Ávila, S.P. Emergence and Evolution of Santa Maria Island (Azores)—The Conundrum of Uplifted Islands Revisited. *Bull. Geol. Soc. Am.* **2017**, *129*, 372–391. [[CrossRef](#)]
53. Costa, A.E. Erosão e Degradação Do Solo Agrícola. *Bol. Da Com. Regul. Dos Cereais* **1952**, *15*, 25–44.
54. Pinheiro, J. Caracterização Geral Dos Solos Da Ilha Terceira (Açores) Que Se Enquadram Na Ordem Andisol. *An. Do Inst. Super. Agron.* **1999**, *47*, 99–117.
55. Ricardo, R.P.; Madeira, M.A.V.; Medina, J.M.B.; Marques, M.M.; Furtado, F.A.S. Esboço Pedológico Da Ilha de S. Miguel (Açores). *An. do Inst. Super. Agron.* **1977**, 275–385.
56. Christenhusz, M.J.M.; Byng, J.W. The number of known plants species in the world and its annual increase. *Phytotaxa* **2016**, *261*, 201–217. [[CrossRef](#)]
57. Quinet, A.; Andreatta, R.H.P. Lauraceae Jussieu Na Reserva Ecológica de Macaé de Cima, Município de Nova Friburgo, Rio de Janeiro, Brasil. *Rodriguesia* **2002**, *53*, 59–121. [[CrossRef](#)]
58. Marques, C.A. Economic Importance of Family Lauraceae Linal. *Floresta E Ambient.* **2001**, *8*, 195–206.
59. Silva, L.; Beech, E. *Laurus azorica*. *The IUCN Red List of Threatened Species 2017: E.T38397A81868030*; IUCN Global Species Programme Red List Unit: Cambridge, UK, 2017.
60. DRRF. *Plano de Gestão Florestal Do Perímetro Florestal e Matas Regionais Da Ilha de São Miguel*; Ponta Delgada: Região Autónoma dos Açores, Portugal, 2017.
61. Speer, J.H. *Fundamentals of Tree-Ring Research*; James, H.S., Ed.; University of Arizona Press: Tucson, AZ, USA, 2010; Volume 26.
62. Schindelin, J.; Arganda-Carreras, I.; Frise, E.; Kaynig, V.; Longair, M.; Pietzsch, T.; Preibisch, S.; Rueden, C.; Saalfeld, S.; Schmid, B.; et al. Fiji: An Open-Source Platform for Biological-Image Analysis. *Nat. Methods* **2012**, *9*, 676–682. [[CrossRef](#)]
63. Schweingruber, F.H. *Tree Rings: Basics and Applications of Dendrochronology*; Kluwer: Dordrecht, The Netherlands, 1988.
64. Buras, A.; Wilmking, M. Correcting the Calculation of Gleichläufigkeit. *Dendrochronologia* **2015**, *34*, 29–30. [[CrossRef](#)]
65. Bunn, A.G. A Dendrochronology Program Library in R (DplR). *Dendrochronologia* **2008**, *26*, 115–124. [[CrossRef](#)]
66. Fritts, H.C. *Tree Rings and Climate*; Academic Press: New York, NY, USA, 1976.
67. Bontemps, J.D.; Esper, J. Statistical Modelling and RCS Detrending Methods Provide Similar Estimates of Long-Term Trend in Radial Growth of Common Beech in North-Eastern France. *Dendrochronologia* **2011**, *29*, 99–107. [[CrossRef](#)]
68. Cook, E.R.; Kairiukstis, L. *Methods of Dendrochronology: Applications in the Environmental Science*; Cook, E.R., Kairiukstis, L.A., Eds.; Springer-Science+Business Media B.V.: Berlin/Heidelberg, Germany, 1990; ISBN 978-90-481-4060-2.
69. Esper, J.; Schneider, L.; Smerdon, J.E.; Schöne, B.R.; Büntgen, U. Signals and Memory in Tree-Ring Width and Density Data. *Dendrochronologia* **2015**, *35*, 62–70. [[CrossRef](#)]
70. Brienen, R.J.W.; Schöngart, J.; Zuidema, P.A. Tree Rings in the Tropics: Insights into the Ecology and Climate Sensitivity of Tropical Trees. In *Tropical Tree Physiology*; Springer: Berlin/Heidelberg, Germany, 2016; pp. 439–461, ISBN 9783319274225.
71. Cook, E.R. *A Time Series Analysis Approach to Tree Ring Standardization*; University of Arizona: Tucson, Arizona, 1985.
72. Cook, E.R.; Pederson, N. *Uncertainty, Emergence, and Statistics in Dendrochronology*; Springer: Dordrecht, The Netherlands, 2011; ISBN 9781402057250.
73. Wigley, T.M.L.; Briffa, K.R.; Jones, P.D. On the Average Value of Correlated Time Series with Applications in Dendroclimatology and Hydrometeorology. *J. Clim. Appl. Meteorol.* **1984**, *23*, 201–213. [[CrossRef](#)]
74. Buras, A. A Comment on the Expressed Population Signal. *Dendrochronologia* **2017**, *44*, 130–132. [[CrossRef](#)]

75. Karger, D.N.; Conrad, O.; Böhner, J.; Kawohl, T.; Kreft, H.; Soria-Auza, R.W.; Zimmermann, N.E.; Linder, P.; Kessler, M. Climatologies at High Resolution for the Earth Land Surface Areas. *Sci. Data* **2017**, *4*, 170122. [[CrossRef](#)]
76. Karger, D.N.; Zimmermann, N.E. CHELSAcruts—High Resolution Temperature and Precipitation Timeseries for the 20th Century and Beyond. *EnviDat* **2018**. [[CrossRef](#)]
77. Jevšenak, J.; Džeroski, S.; Zavadlav, S.; Levanič, T. A Machine Learning Approach to Analyzing the Relationship between Temperatures and Multi-Proxy Tree-Ring Records. *Tree-Ring Res.* **2018**, *74*, 210–224. [[CrossRef](#)]
78. Sahour, H.; Gholami, V.; Torkaman, J.; Vazifedan, M.; Saeedi, S. Random Forest and Extreme Gradient Boosting Algorithms for Streamflow Modeling Using Vessel Features and Tree-Rings. *Environ. Earth Sci.* **2021**, *80*, 1–14. [[CrossRef](#)]
79. Cui, J.P.; Qureshi, S.; Harris, A.; Jim, C.Y.; Wang, H.F. Venerable Trees of Tropical Chinese Wuzhishan City: Distribution Patterns and Drivers. *Urban Ecosyst.* **2022**, *25*, 1765–1776. [[CrossRef](#)]
80. Rossi, S.; Deslauriers, A.; Gričar, J.; Seo, J.W.; Rathgeber, C.B.K.; Anfodillo, T.; Morin, H.; Levanic, T.; Oven, P.; Jalkanen, R. Critical Temperatures for Xylogenesis in Conifers of Cold Climates. *Glob. Ecol. Biogeogr.* **2008**, *17*, 696–707. [[CrossRef](#)]
81. Breiman, L. Random Forests. *Mach. Learn.* **2001**, *45*, 5–32. [[CrossRef](#)]
82. Archer, K.J.; Kimes, R.V. Empirical Characterization of Random Forest Variable Importance Measures. *Comput. Stat. Data Anal.* **2008**, *52*, 2249–2260. [[CrossRef](#)]
83. Li, X.; Chen, G.; Qin, W.; Wang, X.; Liu, H.; Wang, P. Differences in Responses of Tree-Ring $\Delta^{13}C$ in Angiosperms and Gymnosperms to Climate Change on a Global Scale. *For. Ecol. Manag.* **2021**, *492*, 119247. [[CrossRef](#)]
84. Jevšenak, J.; Skudnik, M. A Random Forest Model for Basal Area Increment Predictions from National Forest Inventory Data. *For. Ecol. Manag.* **2021**, *479*, 118601. [[CrossRef](#)]
85. Lucas, T.C.D. A Translucent Box: Interpretable Machine Learning in Ecology. *Ecol. Monogr.* **2020**, *90*, e01422. [[CrossRef](#)]
86. Ávila, S.P.; Cordeiro, R.; Madeira, P.; Silva, L.; Medeiros, A.; Rebelo, A.C.; Melo, C.; Neto, A.I.; Haroun, R.; Monteiro, A.; et al. Global Change Impacts on Large-Scale Biogeographic Patterns of Marine Organisms on Atlantic Oceanic Islands. *Mar. Pollut. Bull.* **2018**, *126*, 101–112. [[CrossRef](#)]
87. Parelho, C.; Rodrigues, A.; Barreto, M. do C.; Cruz, J.V.; Rasche, F.; Silva, L.; Garcia, P. Bioaccumulation and Potential Ecotoxicological Effects of Trace Metals along a Management Intensity Gradient in Volcanic Pasturelands. *Chemosphere* **2021**, *273*, 128601. [[CrossRef](#)]
88. Barreiro, A.; Fox, A.; Jongen, M.; Melo, J.; Musyoki, M.; Vieira, A.; Zimmermann, J.; Carlsson, G.; Cruz, C.; Lüscher, A.; et al. Soil Bacteria Respond to Regional Edapho-Climatic Conditions While Soil Fungi Respond to Management Intensity in Grasslands along a European Transect. *Appl. Soil Ecol.* **2022**, *170*, 104264. [[CrossRef](#)]
89. Sheppard, P.R. Dendroclimatology: Extracting Climate from Trees. *Wiley Interdiscip. Rev. Clim. Chang.* **2010**, *1*, 343–352. [[CrossRef](#)]
90. Johnson, J.B.; Omland, K.S. Model Selection in Ecology and Evolution. *Trends Ecol. Evol.* **2004**, *19*, 101–108. [[CrossRef](#)] [[PubMed](#)]
91. Akaike, H. Maximum Likelihood Identification of Gaussian Autoregressive Moving Average Models. *Biometrika* **1973**, *60*, 255–265. [[CrossRef](#)]
92. Zuur, A.F.; Ieno, E.N.; Smith, G.M. *Analysing Ecological Data*; Springer Science + Business Media, LLC: New York, NY, USA, 2007.
93. Brienen, R.J.W.; Zuidema, P.A. Relating Tree Growth to Rainfall in Bolivian Rain Forests: A Test for Six Species Using Tree Ring Analysis. *Oecologia* **2005**, *146*, 1–12. [[CrossRef](#)] [[PubMed](#)]
94. Espinosa, C.I.; Camarero, J.J.; Gusmán, A.A. Site-Dependent Growth Responses to Climate in Two Major Tree Species from Tropical Dry Forests of Southwest Ecuador. *Dendrochronologia* **2018**, *52*, 11–19. [[CrossRef](#)]
95. Granato-Souza, D.; Adenesky-Filho, E.; Barbosa, A.C.M.C.; Esemann-Quadros, K. Dendrochronological Analyses and Climatic Signals of *Alchornea triplinervia* in Subtropical Forest of Southern Brazil. *Austral Ecol.* **2018**, *43*, 385–396. [[CrossRef](#)]
96. Vasconcellos, T.J.D.; Tomazello-Filho, M.; Callado, C.H. Dendrochronology and Dendroclimatology of *Ceiba speciosa* (A. St.-Hil.) Ravenna (Malvaceae) Exposed to Urban Pollution in Rio de Janeiro City, Brazil. *Dendrochronologia* **2019**, *53*, 104–113. [[CrossRef](#)]
97. Ford, K.R.; Breckheimer, I.K.; Franklin, J.F.; Freund, J.A.; Kroiss, S.J.; Larson, A.J.; Theobald, E.J.; HilleRisLambers, J. Competition Alters Tree Growth Responses to Climate at Individual and Stand Scales. *Can. J. For. Res.* **2017**, *47*, 53–62. [[CrossRef](#)]
98. Zalloni, E.; Battipaglia, G.; Cherubini, P.; Saurer, M.; De Micco, V. Wood Growth in Pure and Mixed *Quercus ilex* L. Forests: Drought Influence Depends on Site Conditions. *Front. Plant Sci.* **2019**, *10*, 397. [[CrossRef](#)]
99. Bhuyan, U.; Zang, C.; Vicente-Serrano, S.M.; Menzel, A. Exploring Relationships among Tree-Ring Growth, Climate Variability, and Seasonal Leaf Activity on Varying Timescales and Spatial Resolutions. *Remote Sens.* **2017**, *9*, 526. [[CrossRef](#)]
100. Lopatin, E.; Kolström, T.; Spiecker, H. Determination of Forest Growth Trends in Komi Republic (Northwestern Russia): Combination of Tree-Ring Analysis and Remote Sensing Data. *Boreal Environ. Res.* **2006**, *11*, 341–353.
101. Babst, F.; Bodesheim, P.; Charney, N.; Friend, A.D.; Girardin, M.P.; Klesse, S.; Moore, D.J.P.; Seftigen, K.; Björklund, J.; Bouriaud, O.; et al. When Tree Rings Go Global: Challenges and Opportunities for Retro- and Prospective Insight. *Quat. Sci. Rev.* **2018**, *197*, 1–20. [[CrossRef](#)]
102. Arlot, S.; Genuer, R. Analysis of Purely Random Forests Bias. *arXiv* **2014**, arXiv:1407.3939.
103. Painsky, A.; Rosset, S. Cross-Validated Variable Selection in Tree-Based Methods Improves Predictive Performance. *IEEE Trans. Pattern Anal. Mach. Intell.* **2017**, *39*, 2142–2153. [[CrossRef](#)] [[PubMed](#)]
104. Pirayonesi, S.M.; El-Diraby, T.E. Role of Data Analytics in Infrastructure Asset Management: Overcoming Data Size and Quality Problems. *J. Transp. Eng. Part B Pavements* **2020**, *146*, 04020022. [[CrossRef](#)]

105. Fox, E.W.; Hill, R.A.; Leibowitz, S.G.; Olsen, A.R.; Thornbrugh, D.J.; Weber, M.H. Assessing the Accuracy and Stability of Variable Selection Methods for Random Forest Modeling in Ecology. *Environ. Monit. Assess.* **2017**, *189*, 316. [\[CrossRef\]](#)
106. Zheng, B.; Agresti, A. Summarizing the Predictive Power of a Generalized Linear Model. *Stat. Med.* **2000**, *19*, 1771–1781. [\[CrossRef\]](#)
107. Dobson, A.J.; Barnett, A.G. *An Introduction to Generalized Linear Models*, 4th ed.; Dobson, A.J., Barnett, A.G., Eds.; CRC Press: Boca Raton, FL, USA, 2018; ISBN 978-1-138-74168-3.
108. Cermák, J.; Jiménez, M.S.; González-Rodríguez, A.M.; Morales, D. Laurel Forests in Tenerife, Canary Islands: II. Efficiency of the Water Conducting System in *Laurus azorica* Trees. *Trees–Struct. Funct.* **2002**, *16*, 538–546. [\[CrossRef\]](#)
109. Tixier, A.; Gambetta, G.A.; Godfrey, J.; Orozco, J.; Zwieniecki, M.A. Non-Structural Carbohydrates in Dormant Woody Perennials; The Tale of Winter Survival and Spring Arrival. *Front. For. Glob. Chang.* **2019**, *2*, 18. [\[CrossRef\]](#)
110. Wong, C.Y.S.; Young, D.J.N.; Latimer, A.M.; Buckley, T.N.; Magney, T.S. Importance of the Legacy Effect for Assessing Spatiotemporal Correspondence between Interannual Tree-Ring Width and Remote Sensing Products in the Sierra Nevada. *Remote Sens. Environ.* **2021**, *265*, 112635. [\[CrossRef\]](#)
111. Körner, C. Carbon Limitation in Trees. *J. Ecol.* **2003**, *91*, 4–17. [\[CrossRef\]](#)
112. Körner, C. Paradigm Shift in Plant Growth Control. *Curr. Opin. Plant Biol.* **2015**, *25*, 107–114. [\[CrossRef\]](#) [\[PubMed\]](#)
113. Prada, S.; Menezes de Sequeira, M.; Figueira, C.; da Silva, M.O. Fog Precipitation and Rainfall Interception in the Natural Forests of Madeira Island (Portugal). *Agric. For. Meteorol.* **2009**, *149*, 1179–1187. [\[CrossRef\]](#)
114. Dias, E.; Melo, C. Factors Influencing the Distribution of Azorean Mountain Vegetation: Implications for Nature Conservation. *Biodivers. Conserv.* **2010**, *19*, 3311–3326. [\[CrossRef\]](#)
115. Dawadi, B.; Liang, E.; Tian, L.; Devkota, L.P.; Yao, T. Pre-Monsoon Precipitation Signal in Tree Rings of Timberline *Betula utilis* in the Central Himalayas. *Quat. Int.* **2013**, *283*, 72–77. [\[CrossRef\]](#)
116. Thapa, U.K.; Shah, S.K.; Gaire, N.P.; Bhujju, D.R. Spring Temperatures in the Far-Western Nepal Himalaya since AD 1640 Reconstructed from *Picea smithiana* Tree-Ring Widths. *Clim. Dyn.* **2015**, *45*, 2069–2081. [\[CrossRef\]](#)
117. Schäfer, H. *Flora of the Azores—A Field Guide*; 2nd ed.; Margraf Publishers: Weikersheim, Duitsland, 2005.
118. Zani, D.; Crowther, T.W.; Mo, L.; Renner, S.S.; Zohner, C.M. Increased Growing-Season Productivity Drives Earlier Autumn Leaf Senescence in Temperate Trees. *Science* **2020**, *37*, 1066–1071. [\[CrossRef\]](#)
119. Babst, F.; Bouriaud, O.; Poulter, B.; Trouet, V.; Girardin, M.P.; Frank, D.C. Twentieth Century Redistribution in Climatic Drivers of Global Tree Growth. *Sci. Adv.* **2019**, *5*, eaat4313. [\[CrossRef\]](#)
120. Harvey, J.E.; Smiljanić, M.; Scharnweber, T.; Buras, A.; Cedro, A.; Cruz-García, R.; Drobyshev, I.; Janecka, K.; Jansons, Ā.; Kaczka, R.; et al. Tree Growth Influenced by Warming Winter Climate and Summer Moisture Availability in Northern Temperate Forests. *Glob. Chang. Biol.* **2020**, *26*, 2505–2518. [\[CrossRef\]](#)
121. Weijers, S.; Pape, R.; Löffler, J.; Myers-Smith, I.H. Contrasting Shrub Species Respond to Early Summer Temperatures Leading to Correspondence of Shrub Growth Patterns. *Environ. Res. Lett.* **2018**, *13*, 034005. [\[CrossRef\]](#)
122. Zhang, L.; Jiang, Y.; Zhao, S.; Jiao, L.; Wen, Y. Relationships between Tree Age and Climate Sensitivity of Radial Growth in Different Drought Conditions of Qilian Mountains, Northwestern China. *Forests* **2018**, *9*, 135. [\[CrossRef\]](#)
123. Biondi, F. Are Climate-Tree Growth Relationships Changing in North-Central Idaho, U.S.A.? *Arct. Antarct. Alp. Res.* **2000**, *32*, 111–116. [\[CrossRef\]](#)
124. Fritts, H.C. Growth-Rings of Trees: Their Correlation with Climate. *Science* **1966**, *154*, 973–979. [\[CrossRef\]](#) [\[PubMed\]](#)
125. Qaderi, M.M.; Martel, A.B.; Dixon, S.L. Environmental Factors Influence Plant Vascular System and Water Regulation. *Plants* **2019**, *8*, 65. [\[CrossRef\]](#) [\[PubMed\]](#)
126. Roig-Oliver, M.; Fullana-Pericàs, M.; Bota, J.; Flexas, J. Adjustments in Photosynthesis and Leaf Water Relations Are Related to Changes in Cell Wall Composition in *Hordeum vulgare* and *Triticum aestivum* Subjected to Water Deficit Stress. *Plant Sci.* **2021**, *311*, 111015. [\[CrossRef\]](#) [\[PubMed\]](#)
127. Gonçalves, J.Q.; Durgante, F.M.; Wittmann, F.; Teresa, M.; Piedade, F.; Ricardo, D.; Rodriguez, O.; Tomazello, M.; Pia, F.; Schöngart, J. Minimum Temperature and Evapotranspiration in Central Amazonian Floodplains Limit Tree Growth of *Nectandra amazonum* (Lauraceae). *Trees* **2021**, *35*, 1367–1384. [\[CrossRef\]](#)
128. Sun, M.; Li, J.; Cao, R.; Tian, K.; Zhang, W.; Yin, D.; Zhang, Y. Climate-Growth Relations of *Abies Georgei* along an Altitudinal Gradient in Haba Snow Mountain, Southwestern China. *Forests* **2021**, *12*, 1569. [\[CrossRef\]](#)
129. Camarero, J.J.; Rubio-Cuadrado, A. Relating Climate, Drought and Radial Growth in Broadleaf Mediterranean Tree and Shrub Species: A New Approach to Quantify Climate-Growth Relationships. *Forests* **2020**, *11*, 1250. [\[CrossRef\]](#)
130. Roibu, C.C.; Sfecla, V.; Mursa, A.; Ionita, M.; Nagavciuc, V.; Chirilaoei, F.; Lesan, I.; Popa, I. The Climatic Response of Tree Ring Width Components of Ash (*Fraxinus excelsior* L.) and Common Oak (*Quercus robur* L.) from Eastern Europe. *Forests* **2020**, *11*, 600. [\[CrossRef\]](#)
131. Anderson-Teixeira, K.J.; Herrmann, V.; Rollinson, C.R.; Gonzalez, B.; Gonzalez-Akre, E.B.; Pederson, N.; Alexander, M.R.; Allen, C.D.; Alfaro-Sánchez, R.; Awada, T.; et al. Joint Effects of Climate, Tree Size, and Year on Annual Tree Growth Derived from Tree-Ring Records of Ten Globally Distributed Forests. *Glob. Chang. Biol.* **2022**, *28*, 245–266. [\[CrossRef\]](#)
132. Boninsegna, J.A.; Argollo, J.; Aravena, J.C.; Barichivich, J.; Christie, D.; Ferrero, M.E.; Lara, A.; Le Quesne, C.; Luckman, B.H.; Masiokas, M.; et al. Dendroclimatological Reconstructions in South America: A Review. *Palaeogeogr. Palaeoclimatol. Palaeoecol.* **2009**, *281*, 210–228. [\[CrossRef\]](#)

133. Babst, F.; Poulter, B.; Trouet, V.; Tan, K.; Neuwirth, B.; Wilson, R.; Carrer, M.; Grabner, M.; Tegel, W.; Levanic, T.; et al. Site- and Species-Specific Responses of Forest Growth to Climate across the European Continent. *Glob. Ecol. Biogeogr.* **2013**, *22*, 706–717. [[CrossRef](#)]
134. Hacket-Pain, A.J.; Friend, A.D.; Lagueard, J.G.A.; Thomas, P.A. The Influence of Masting Phenomenon on Growth-Climate Relationships in Trees: Explaining the Influence of Previous Summers' Climate on Ring Width. *Tree Physiol.* **2015**, *35*, 319–330. [[CrossRef](#)] [[PubMed](#)]
135. Xu, G.; Wu, G.; Liu, X.; Chen, T.; Wang, B.; Hudson, A.; Trouet, V. Age-Related Climate Response of Tree-Ring $\Delta^{13}\text{C}$ and $\Delta^{18}\text{O}$ From Spruce in Northwestern China, With Implications for Relative Humidity Reconstructions. *J. Geophys. Res. Biogeosci.* **2020**, *125*, 1–18. [[CrossRef](#)]
136. Timofeeva, G.; Treydte, K.; Bugmann, H.; Rigling, A.; Schaub, M.; Siegwolf, R.; Saurer, M. Long-Term Effects of Drought on Tree-Ring Growth and Carbon Isotope Variability in Scots Pine in a Dry Environment. *Tree Physiol.* **2017**, *37*, 1028–1041. [[CrossRef](#)] [[PubMed](#)]
137. LaMarche, V.C.; Stockton, C.W. Chronologies from Temperature-Sensitive Bristlecone Pines at Upper Treeline in Western United States. *Tree-Ring Bull.* **1974**, *34*, 21–45.
138. Szejner, P.; Wright, W.E.; Belmecheri, S.; Meko, D.; Leavitt, S.W.; Ehleringer, J.R.; Monson, R.K. Disentangling Seasonal and Interannual Legacies from Inferred Patterns of Forest Water and Carbon Cycling Using Tree-Ring Stable Isotopes. *Glob. Chang. Biol.* **2018**, *24*, 5332–5347. [[CrossRef](#)]
139. Smith, M.G.; Miller, R.E.; Arndt, S.K.; Kasel, S.; Bennett, L.T. Whole-Tree Distribution and Temporal Variation of Non-Structural Carbohydrates in Broadleaf Evergreen Trees. *Tree Physiol.* **2018**, *38*, 570–581. [[CrossRef](#)]
140. Kannenberg, S.A.; Maxwell, J.T.; Pederson, N.; D'Orangeville, L.; Ficklin, D.L.; Phillips, R.P. Drought Legacies Are Dependent on Water Table Depth, Wood Anatomy and Drought Timing across the Eastern US. *Ecol. Lett.* **2019**, *22*, 119–127. [[CrossRef](#)]
141. Liu, W.; Su, J.; Li, S.; Lang, X.; Huang, X. Non-Structural Carbohydrates Regulated by Season and Species in the Subtropical Monsoon Broad-Leaved Evergreen Forest of Yunnan Province, China. *Sci. Rep.* **2018**, *8*, 1–10. [[CrossRef](#)]
142. Monserud, R.A.; Marshall, J.D. Time-Series Analysis of $\Delta^{13}\text{C}$ from Tree Rings. I. Time Trends and Autocorrelation. *Tree Physiol.* **2001**, *21*, 1087–1102. [[CrossRef](#)]
143. McCarroll, D.; Whitney, M.; Young, G.H.F.; Loader, N.J.; Gagen, M.H. A Simple Stable Carbon Isotope Method for Investigating Changes in the Use of Recent versus Old Carbon in Oak. *Tree Physiol.* **2017**, *37*, 1021–1027. [[CrossRef](#)] [[PubMed](#)]
144. Primicia, I.; Camarero, J.J.; Janda, P.; Čada, V.; Morrissey, R.C.; Trotsiuk, V.; Bače, R.; Teodosiu, M.; Svoboda, M. Age, Competition, Disturbance and Elevation Effects on Tree and Stand Growth Response of Primary *Picea abies* Forest to Climate. *For. Ecol. Manag.* **2015**, *354*, 77–86. [[CrossRef](#)]
145. Lu, K.; Chen, N.; Zhang, C.; Dong, X.; Zhao, C. Drought Enhances the Role of Competition in Mediating the Relationship between Tree Growth and Climate in Semi-Arid Areas of Northwest China. *Forests* **2019**, *10*, 804. [[CrossRef](#)]
146. Moser-Reischl, A.; Rahman, M.A.; Pauleit, S.; Pretzsch, H.; Rötzer, T. Growth Patterns and Effects of Urban Micro-Climate on Two Physiologically Contrasting Urban Tree Species. *Landsc. Urban Plan.* **2019**, *183*, 88–99. [[CrossRef](#)]
147. Wang, B.; Yu, P.; Yu, Y.; Wan, Y.; Wang, Y.; Zhang, L.; Wang, S.; Wang, X.; Liu, Z.; Xu, L. Effects of Canopy Position on Climate-Growth Relationships of Qinghai Spruce in the Central Qilian Mountains, Northwestern China. *Dendrochronologia* **2020**, *64*, 125756. [[CrossRef](#)]
148. Yang, J.; Cooper, D.J.; Li, Z.; Song, W.; Zhang, Y.; Zhao, B.; Han, S.; Wang, X. Differences in Tree and Shrub Growth Responses to Climate Change in a Boreal Forest in China. *Dendrochronologia* **2020**, *63*, 125744. [[CrossRef](#)]
149. Foster, J.R.; Finley, A.O.; D'Amato, A.W.; Bradford, J.B.; Banerjee, S. Predicting Tree Biomass Growth in the Temperate-Boreal Ecotone: Is Tree Size, Age, Competition, or Climate Response Most Important? *Glob. Chang. Biol.* **2016**, *22*, 2138–2151. [[CrossRef](#)]
150. Rollinson, C.R.; Kaye, M.W.; Canham, C.D. Interspecific Variation in Growth Responses to Climate and Competition of Five Eastern Tree Species. *Ecology* **2016**, *97*, 1003–1011. [[CrossRef](#)]
151. van der Maaten-Theunissen, M.; Bouriaud, O. Climate-Growth Relationships at Different Stem Heights in Silver Fir and Norway Spruce. *Can. J. For. Res.* **2012**, *42*, 958–969. [[CrossRef](#)]
152. Mazza, G.; Gallucci, V.; Manetti, M.C.; Urbinati, C. Climate-Growth Relationships of Silver Fir (*Abies alba* Mill.) in Marginal Populations of Central Italy. *Dendrochronologia* **2014**, *32*, 181–190. [[CrossRef](#)]
153. Misi, D.; Puchałka, R.; Pearson, C.; Robertson, I.; Koprowski, M. Differences in the Climate-Growth Relationship of Scots Pine: A Case Study from Poland and Hungary. *Forests* **2019**, *10*, 243. [[CrossRef](#)]
154. Sun, Y.; Henderson, M.; Liu, B.; Yan, H. Directional Variability in Response of *Pinus koraiensis* Radial Growth to Climate Change. *Forests* **2021**, *12*, 1684. [[CrossRef](#)]
155. Benito Garzón, M.; Robson, T.M.; Hampe, A. Δ TraitSDMs: Species Distribution Models That Account for Local Adaptation and Phenotypic Plasticity. *New Phytol.* **2019**, *222*, 1757–1765. [[CrossRef](#)] [[PubMed](#)]
156. Kumarathunge, D.P.; Medlyn, B.E.; Drake, J.E.; Tjoelker, M.G.; Aspinwall, M.J.; Battaglia, M.; Cano, F.J.; Carter, K.R.; Cavaleri, M.A.; Cernusak, L.A.; et al. Acclimation and Adaptation Components of the Temperature Dependence of Plant Photosynthesis at the Global Scale. *New Phytol.* **2019**, *222*, 768–784. [[CrossRef](#)]
157. Wright, S.J.; Goad, D.M.; Gross, B.L.; Muñoz, P.R.; Olsen, K.M. Genetic Trade-Offs Underlie Divergent Life History Strategies for Local Adaptation in White Clover. *Mol. Ecol.* **2022**, *31*, 3742–3760. [[CrossRef](#)]

158. Ren, L.; Guo, X.; Liu, S.; Yu, T.; Guo, W.; Wang, R.; Ye, S.; Lambertini, C.; Brix, H.; Eller, F. Intraspecific Variation in *Phragmites australis*: Clonal Adaption of Functional Traits and Phenotypic Plasticity Vary with Latitude of Origin. *J. Ecol.* **2020**, *108*, 2531–2543. [[CrossRef](#)]
159. Souto-Herrero, M.; Rozas, V.; García-González, I. Earlywood Vessels and Latewood Width Explain the Role of Climate on Wood Formation of *Quercus pyrenaica* Willd. across the Atlantic-Mediterranean Boundary in NW Iberia. *For. Ecol. Manag.* **2018**, *425*, 126–137. [[CrossRef](#)]
160. García-González, I.; Fonti, P. Selecting Earlywood Vessels to Maximize Their Environmental Signal. *Tree Physiol.* **2006**, *26*, 1289–1296. [[CrossRef](#)]

Disclaimer/Publisher’s Note: The statements, opinions and data contained in all publications are solely those of the individual author(s) and contributor(s) and not of MDPI and/or the editor(s). MDPI and/or the editor(s) disclaim responsibility for any injury to people or property resulting from any ideas, methods, instructions or products referred to in the content.